Computational Fluid Dynamic Optimization of an Experimental Rotating Detonation Rocket Engine Nozzle

Daniel E. Paxson[1], Kenji Miki[2], H. Douglas Perkins[3]
NASA Glenn Research Center, Cleveland, Ohio, 44135, USA

Shaye Yungster[4]
HX5, LLC, Cleveland, Ohio, 44142, USA

A parametric optimization study is performed on the nozzle of a laboratory rotating detonation rocket engine (RDRE) using a three-dimensional computational fluid dynamic simulation. The primary optimization objective is maximum nozzle thrust. The basic nozzle configuration is a shrouded, truncated plug. The fluid in the RDRE chamber leading to the nozzle is choked at its exit so that its cyclic behavior is unaffected by any changes to the nozzle design. Optimization is performed for a single operating point. Parameters varied are the overall nozzle area expansion ratio and the fraction of the expansion area that is provided by the shroud. These two parameters indirectly affect the angle of the plug nozzle cone, and the bluff body area associated with its truncation. Nozzle thrust is evaluated as the difference between the thrust of the RDRE chamber-plus-nozzle combination and that of the chamber alone. The nozzle produces approximately 20% of the total engine thrust. The baseline nozzle is found to perform well, yielding 58.1% of the thrust calculated for a notional ideal RDRE nozzle which can instantaneously change shape to allow isentropic expansion of every fluid element. Optimization improves the performance, bringing the nozzle thrust to 70.0% of the notional ideal, and total engine thrust (chamber-plus-nozzle) to 94% of the ideal.

Nomenclature

A	=	cross-sectional area
F	=	thrust force
M	=	Mach number
P	=	total pressure
p	=	static pressure
R_g	=	specific gas constant
T	=	temperature
t	=	time
v	=	velocity
x	=	normalized azimuthal distance
y	=	normalized axial distance

Greek

γ	=	ratio of specific heats

[1] Aerospace Research Engineer, Research and Engineering Directorate, AIAA Associate Fellow.
[2] Aerospace Research Engineer, Research and Engineering Directorate, AIAA Senior Member
[3] Aerospace Research Engineer, Research and Engineering Directorate, AIAA Senior Member
[4] Aerospace Research Engineer, Research and Engineering Directorate, AIAA Senior Member

ρ = density

Subscripts
amb = ambient
axial = axial component
ch = channel
cycle = limit cycle
e = exit plane
i = ideal
m = inlet manifold
n = nozzle
no_nozzle = without a nozzle
sh = shroud

I. Introduction

The pressure gain combustion (PGC) community is currently investigating the application of rotating detonation rocket engines (RDRE) for space propulsion. If successful, RDREs could lead to highly compact propulsion systems that deliver high specific impulse at substantially lower pump discharge pressure when compared to conventional rocket engines. The typical RDRE consists of an annular channel with a fluidic valve at one end (i.e., promoting forward flow and resisting backflow) and a nozzle at the other end. Fuel and oxidizer enter axially through the valved end. The detonation wave travels circumferentially at supersonic speeds. Combustion products exit predominantly axially through the open end. Most of the fluid entering the device is passed over by the rotating detonation wave which, as a form of confined heat release, substantially raises the pressure and temperature. The fluid is then expanded and accelerated as it travels down the annulus. Further expansion and thrust production occur in the nozzle. Detailed descriptions of operation are abundant in the literature (e.g., Refs. 1 and 2).

In principle, the flow exiting the device has a higher average total pressure than the flow that enters. In practice, achieving this so-called pressure gain is a formidable challenge. RDRE flow fields are remarkably complex. There are multiple length and time scales to consider along with multiple fluid states. Furthermore, RDREs are fundamentally unsteady, which means that most of the design rules for conventional steady rocket engines do not apply.

One area where this is particularly relevant is the RDRE exhaust nozzle. There are currently few design guidelines available. The annular channel geometry makes a truncated plug nozzle the most obvious choice for the basic nozzle configuration [3, 4]. However, the unsteady and spatially non-uniform flow field supplying such a nozzle renders common nozzle parameters such as pressure ratio, and throat Mach number ill-defined. And while there is no net swirl in the RDRE exit flow, there are significant local tangential velocity components. Additionally, there are unsteady boundary layers in the nozzle that can lead to unpredictable flow paths. These and other factors make RDRE nozzle design a challenge.

In order to address this challenge a relatively fast computational nozzle design methodology was developed [5] which is applicable to both the RDRE and the air breathing rotating detonation engine (RDE). In this approach, the computational domain is divided into two parts: the annular combustor region and the nozzle section. In the combustor region, a validated quasi-two-dimensional (Q2D) in-house code [6-9] is utilized to generate an unsteady RDRE flow field solution that executes a limit cycle. This flow field can include multiple rotating detonation waves (which are typical in RDREs). The exit plane boundary condition for the combustor region ensures that the flow is sonic or supersonic at all times. The unsteady but periodic flow data at the exit of the annular combustor region is then converted into unsteady and spatially distributed inflow boundary conditions that are used to compute the flow field in the nozzle section. The flow in the nozzle section is computed using the three-dimensional (3D) OpenNCC code developed at the NASA Glenn Research Center [10]. This approach is significantly faster than computing the entire annular combustor and nozzle flow field in the 3D code. This is because the number of grid points needed can be reduced substantially, and because the chemically reacting region of the flow, with its additional species conservation equations, is modeled in the Q2D code with a simple global reaction mechanism. The result is a simulation which allows the exploration of a wide variety of nozzle geometries in a relatively short amount of time.

The present work focuses on applying the Ref. [5] methodology toward optimizing a nozzle for a particular RDRE [11]. This is an approximately 5,000 lb_f experimental engine currently in fabrication at the NASA Marshall Space Flight Center. The test article is intended for the investigation of several critical RDRE technologies including injector design, cooling requirements, and nozzle design. The use of additive manufacturing (AM) to advance these

technologies is also under investigation. The experiment is being developed in partnership with INSpace, LLC under NASA's Announcement of Cooperative Opportunities program. The nozzles detailed in this report will be fabricated and tested on this article. Initial RDRE testing is planned for the 2022 calendar year.

The annular RDRE combustion section is first described, and the computed flow field is presented. The baseline nozzle design, and computed performance thereof are then described. It is shown that the baseline nozzle design performs well, yielding thrust that is 58.1% of an idealized maximum computed via the technique described in [12]. The baseline design is then perturbed by altering two of its geometric parameters: the overall nozzle area expansion ratio, A_e/A_{ch} and the fraction of the expansion area that is provided by the shroud, A_{sh}/A_e. The parameters and methods of perturbation are illustrated. Results from several perturbations are shown. It is found that RDRE nozzle thrust can be improved to 70.0% of the ideal by maintaining the baseline A_e/A_{ch} value of 5 while increasing A_{sh}/A_e from 0.0 to 0.20. The top performing nozzle design is simulated with a refined numerical grid in order to more accurately capture boundary layer phenomena and confirm grid independence of the thrust calculations. The results do not change. The described effort enhances the understanding of nozzle design for RDREs and RDEs and demonstrates the utility of the Ref. 5 methodology.

II. RDRE Description

The RDRE under investigation is shown in Fig. 1 along with the baseline nozzle. Relevant dimensions are listed in the figure. The unit runs on gaseous methane and liquid oxygen. It is designed to nominally flow 17.7 lb_m/s at an equivalence ratio of 1.3. The walls are cooled and are maintained at 1460 R. The experiment is designed to run in the open air, so the nozzle exits to ambient pressure at 14.7 psia. The annulus does not have a physical throat. However, the fluid mechanics of the RDRE still yields sonic or supersonic flow in the annulus exit plane.

A. Q2D Code Annulus Flow Field Solution

The Q2D code used to compute the RDRE annulus flow field is a high-resolution algorithm that integrates the quasi-two-dimensional, two-species, reactive Euler equations with source terms. Details may be found in the literature [2, 6-9]. In brief, the code adopts the detonation frame of reference and deliberately utilizes a coarse grid (i.e., it is diffusive) to eliminate the highest frequency unsteadiness (e.g., detonation cells, Kelvin-Helmholtz phenomena). The result is a flow field solution that is invariant with time when converged. The working fluid is assumed to be a single, calorically perfect gas (CPG). The source terms contain sub-models which govern the reaction rate, momentum losses due to skin-friction, and the effects of heat transfer to the walls.

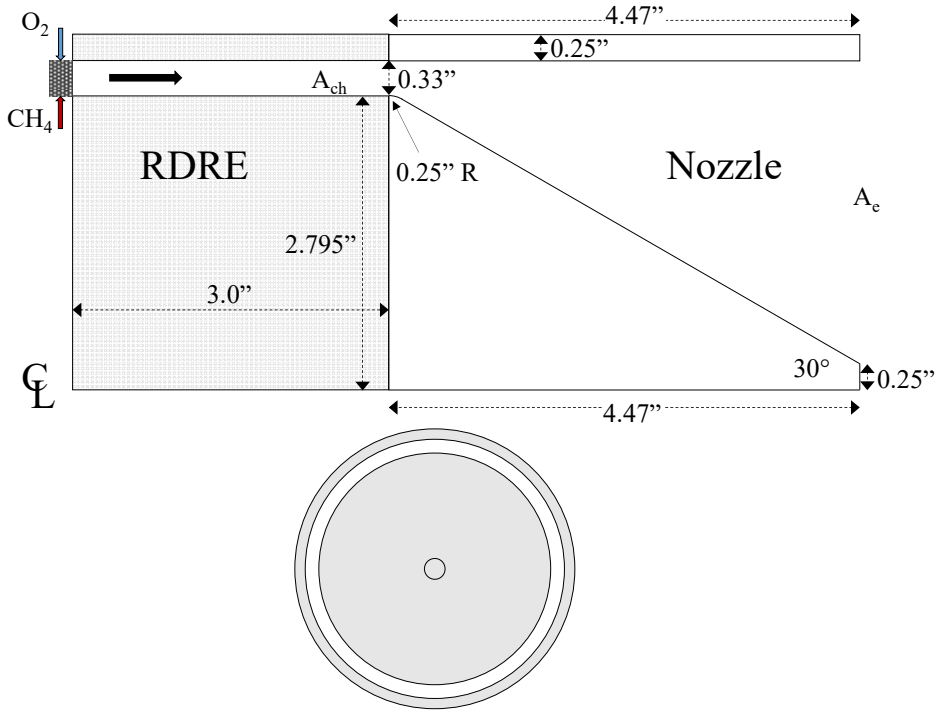

Fig. 1 Schematic of RDRE annulus and baseline nozzle with dimensions, side view (upper); end view (lower)

The governing equations are integrated numerically in time using an explicit, second-order, two-step, Runge-Kutta technique. Spatial flux derivatives are approximated as flux differences, with the fluxes at the discrete cell faces evaluated using Roe's approximate Riemann solver. Second-order spatial accuracy (away from discontinuities) is obtained using piecewise linear representations of the primitive variable states within the cells. Oscillatory behavior is avoided by limiting the linear slopes.

Considering an 'unwrapped' RDE where the non-dimensional circumferential direction is x, and the axial direction is y, the following boundary conditions are imposed. At x=0.0 and x=1.0, periodic conditions are used. These ensure that the x-dimension of the computational space faithfully represents an annulus (which is continuous and has no boundary). At the exit plane, constant pressure outflow is imposed along with characteristic equations to obtain density and axial velocity for the image cells. If the resulting flow is sonic, or supersonic, then the imposed pressure is disregarded. If, in addition, the upstream flow is supersonic, then pressure, density, and axial velocity are extrapolated from the interior. At y=0.0 (the inflow face), several boundary condition options are possible. Since details of the propellant injection scheme were not known when the present investigation began, idealized inflow boundary conditions are used. The inlet face is assumed to be fed by a large manifold at a fixed total pressure, and temperature. If the interior pressure is less than the manifold pressure, P_m then isentropic inflow occurs. If the interior pressure is greater than P_m, as might be found just behind the detonation, then a solid wall boundary condition is applied which simulates a check-valve and prevents backflow. The manifold pressure used is 320 psia. This value was obtained from a preliminary estimate of what would be needed to produce the design mass flow rate. The estimate was made using the simplified RDRE performance model described in Ref. 13. The CPG gas constant, R_g, and ratio of specific heats, γ, were obtained from the same model. The values are 60.12 ft·lb$_f$/lb$_m$·R, and 1.182 respectively. The grid used is 400 × 65 uniformly spaced cells. Two waves are assumed present in the solution. The manifold temperature, T_m, is assumed to be 540 R, and the annulus exits to ambient pressure at 14.7 psia.

The resulting flow field solution is shown in Fig. 2. Contours of temperature are displayed at a moment in time in an unwrapped rendering of the computational space. The computed mass flow rate is 19.1 lb$_m$/s and the ideal thrust, F_i is 5592 lb$_f$. The computed detonation velocity is found to be 82% of the theoretical Chapman-Jouguet value. For reference, the ideal thrust is found by isentropically expanding (i.e. accelerating) each element of mass in the exit plane to its velocity at atmospheric pressure. The axial components of the ideal velocities are then mass flux averaged to obtain an ideal specific thrust which is then multiplied by the computed flow rate to get ideal thrust [12]. Note that this ideal is notional only since it would require a nozzle with variable exit area in both time and space. It predicts higher thrust than could be achieved with a fixed nozzle.

The mass flow rate and ideal thrust values are both slightly higher than initial estimates. However, both are reduced when the exiting flow is converted from the assumed single CPG of the Q2D code to a thermally perfect mixture as required for input by the 3D OpenNCC code.

An equilibrium reaction calculation is performed on the specified fuel and oxidizer mixture using the NASA Chemical Equilibrium with Applications (CEA) software [14]. The fluid state for this calculation is the time-averaged exit pressure and temperature from the CPG code. CEA yields the product composition in constituent mole fractions (constituents are limited to H_2, H_2O, CO_2, and CO). These are used to calculate a mixture gas constant, which is different from that used under the CPG assumption. For this case it is R_g=71.05 ft·lb$_f$/lb$_m$·R. This change lowers the density of flow leaving the annulus and thus reduces both the predicted mass flow rate and ideal thrust. The values become 16.13 lb$_m$/s and F_i=5003 lb$_f$ respectively. The calculated thrust that the annulus would produce without a nozzle, F_{no_nozzle} is 3993 lb$_f$. This is 20% below the ideal thrust and does not include the substantial bluff body drag that would arise if no nozzle were present. The result indicates that, if properly designed, the nozzle contribution to the total thrust is significant.

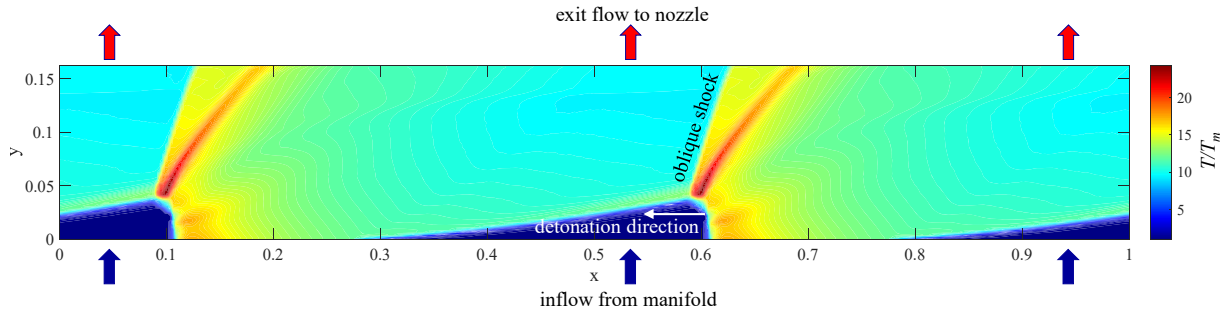

Fig. 2 Contours of temperature in the RDRE annular combustion section at a moment in time

Circumferential distributions of exit plane pressure, temperature, and Mach number (comprised of both axial and circumferential velocity components) from the Fig. 2 calculation using the CEA obtained gas constant are shown in Fig. 3. It is evident that there are large spatial fluctuations in the fluid state. Noting Figs. 2 and 3 represent a moment in time, and that this distribution rotates around the annulus at the detonation velocity of 7,557 ft/s, it is also evident that the exit flow has large temporal fluctuations as well.

As discussed earlier, this rotating distribution at the annulus exit plane was used as an unsteady (but periodic) inlet boundary condition for the 3D simulation of the nozzle section to be discussed. The inlet flow was assumed radially uniform. The process of mapping output from one code into input for another is outlined in Ref. [5].

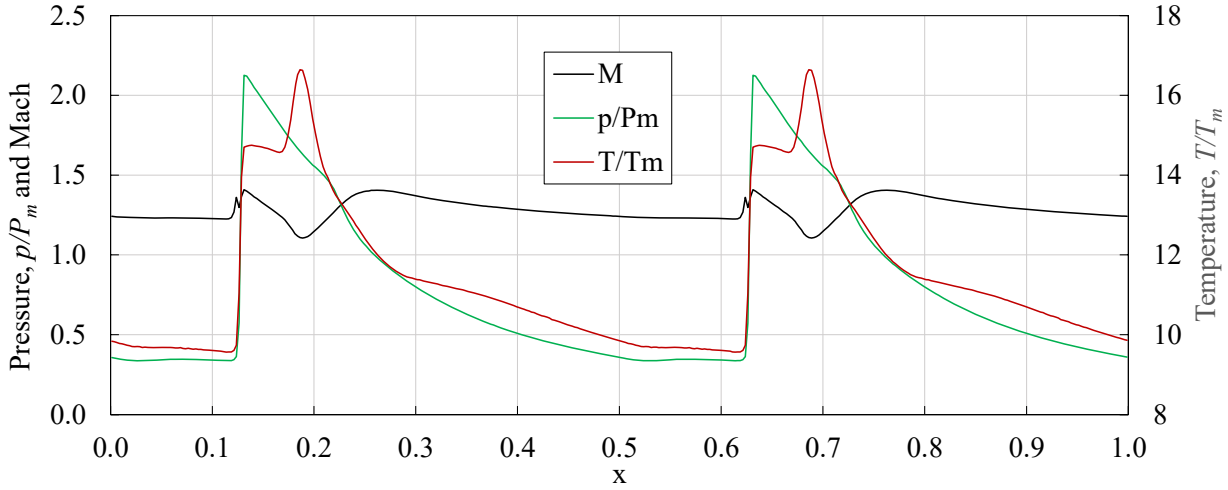

Fig. 3 Circumferential distributions of pressure, temperature, and Mach number in the exit plane of the RDRE annular combustion section at a moment in time

B. 3D Code Baseline Nozzle Solution

Details of the 3D OpenNCC code may be found in the literature [5, 15]. As such, no description will be provided herein beyond stating that it is a robust, multi-species, reacting, unsteady Reynolds averaged Navier Stokes code that has been validated on numerous flow fields. This includes flows with shocks and detonations. No reactions are utilized for this work. The fluid constituent species are 'frozen' throughout the domain.

A rendering of the computational domain and grid used for the simulation is shown in Fig. 4. It contains approximately 4 million numerical cells. It is noted that the nozzle domain contains a small length of the combustor annulus (0.6 in.). This implies that the boundary conditions extracted from the Q2D simulation should have been taken from some distance upstream of the exit plane rather than at the exit plane itself. However, an examination of the fluid states 0.6 in. upstream from the exit plane of Fig. 2 revealed that the distributions differed from those of Fig. 3 by less than 6% as measured by ratios of their standard deviations. This small difference is unlikely to significantly change the nozzle performance; particularly when it is noted that the standard deviations themselves were approximately 70% of the means.

The computational domain was initially filled with CO_2 at ambient conditions. The mapped boundary conditions of Fig. 3 were then imposed on the left face of Fig. 4b and the simulation was run until a limit cycle formed in the nozzle exit plane mass flow rate, the cycle averaged thrust remained constant, and the cycle averaged mass flow rates into and out of the nozzle matched. The boundary condition applied to all surfaces external to the nozzle was a constant pressure of p_{amb}=14.7 psia. Approximately 15 wave revolutions were required for a limit cycle to develop. This was typically obtained in 1.5 days, running on 360 cores (Intel Xeon E5-2680v2 processors) at the NASA Advanced Supercomputing (NAS) facility.

Figure 5 shows contours of pressure in the nozzle at one instant of time after a limit cycle was obtained. The upper contour represents an axial/circumferential surface at a radius that is midway across the annular channel. The lower three contours represent radial/circumferential contours at the three axial locations indicated by the arrows. It is evident from the upper contour that the oblique shocks which originate at the top of the Fig. 2 detonations propagate through the full length of the nozzle. However, they do weaken considerably in the expanding section of the nozzle. The lower contours show the oblique waves transitioning from a form that is uniform in the radial direction to one

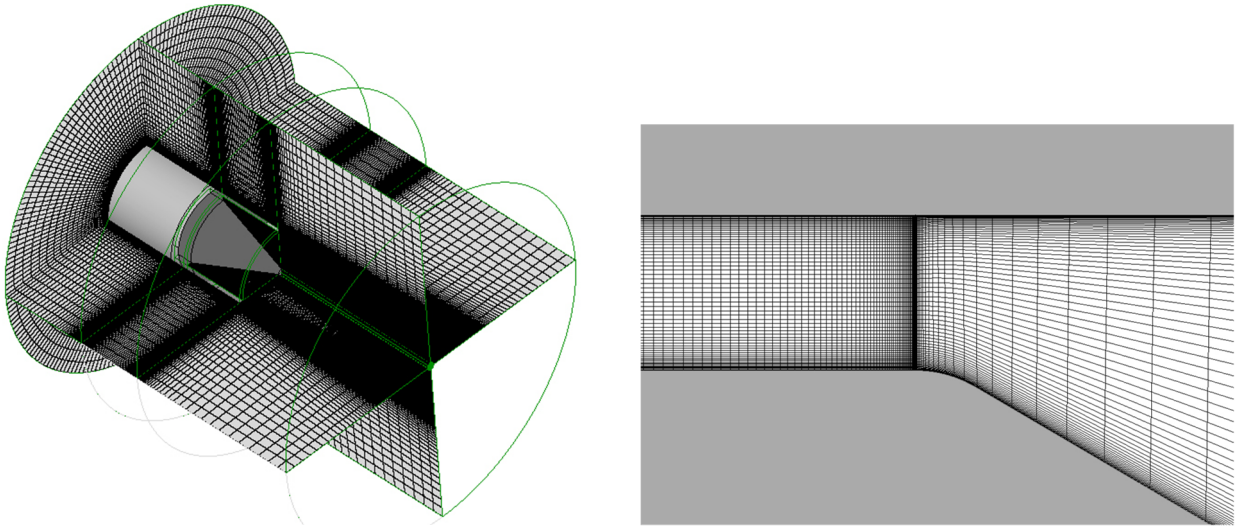

(a) (b)

Fig. 4 RDRE nozzle computational domain and grid (a) and grid detail around the nozzle cone shoulder (b)

that is radially distorted as they travel downstream. It is not clear why this occurs or what impact it has on performance. Further investigation is warranted, but it is beyond the scope of the present effort. It is clear from the Fig. 5 pressure contours however, that the fundamentally unsteady, multi-dimensional phenomena associated with RDRE flow fields require the 3D CFD analysis described in this work in order to accurately assess performance.

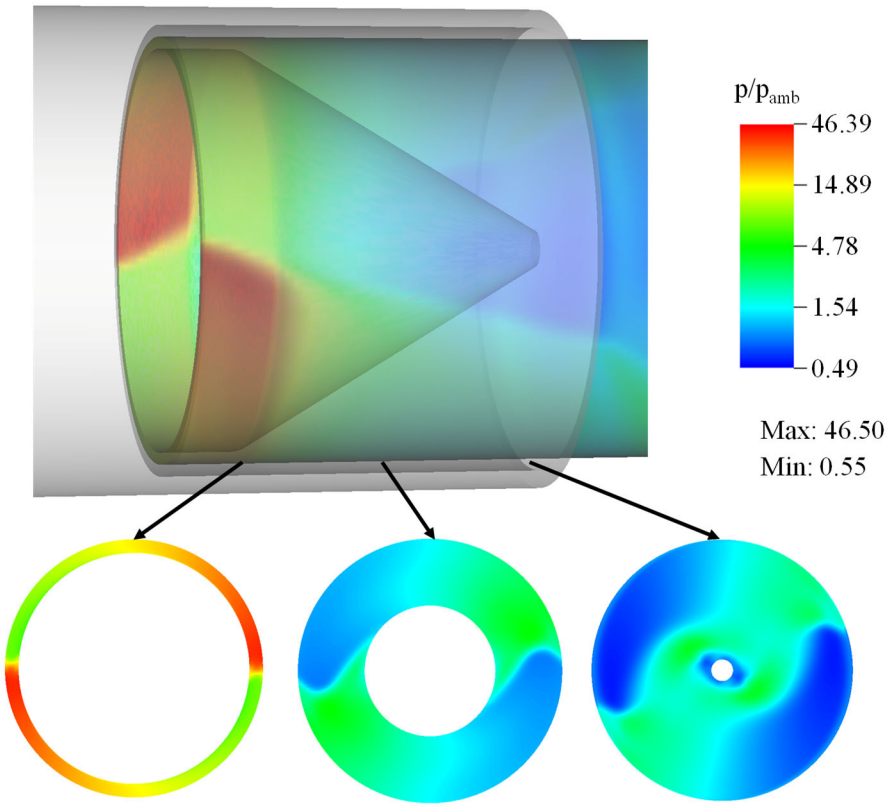

Fig. 5 Contours of pressure (log scale) at a moment in time for the baseline nozzle during limit cycle operation

The total thrust produced by the nozzle and the upstream RDRE annular combustor is 4580 lb_f. This is just 8.5% below the ideal thrust calculated earlier. Total thrust was assessed by computing the cycle time-averaged contributions from momentum and pressure in the nozzle exit plane.

$$F = \frac{1}{t_{cycle}}\left[\iint \rho_e v_{e\_axial}^2 dA_e dt + \iint (p_e - p_{amb}) dA_e dt\right] \quad (1)$$

The cycle time is the time it takes for one of the two waves present to travel the circumference of the RDRE. The time and area averaged pressure in the exit plane is just 6 psig above ambient and provides just 4.3% of the total thrust. This suggests that the flow is only slightly under expanded, at least on an averaged basis. This result was somewhat expected because some preliminary analysis was performed for the baseline nozzle before it was configured for simulation. The analysis was based on steady flow arguments; however, it still proved useful as a preliminary design tool. The ideal specific thrust from the RDRE is used along with the exhausted total enthalpy to calculate its ideal exhaust Mach number of 2.94 [12]. Standard compressible flow equations are then used to determine the ratio of exit area to throat area required to achieve this Mach number (assuming that the throat Mach number is 1.0) [16]. For γ=1.182, the value is A_{e_i}/A_{ch}=6.54. This is just 31% larger than the actual A_e/A_{ch} value of 5.0 for the baseline configuration. Noting that at these conditions a 31% difference in area ratio is associated with only a 4% difference in specific thrust, it was anticipated that the baseline configuration would yield performance that was reasonably close to the ideal.

It is noted in passing that there was another factor in the choice of the baseline configuration. It represents the most compact implementation of a shrouded plug nozzle in terms overall diameter and weight. This also implies minimized cooling requirements. These characteristics could make it the most practical configuration even if it is not the highest performing.

Figure 6 shows the contours of time averaged pressure and Mach number for the baseline nozzle configuration. They indicate that the flow is attached throughout the nozzle (except a small region near the tip of the plug). They also indicate that the vast majority of thrust from the nozzle proper occurs near the plug outer diameter (i.e., the initial expansion region). This region has the highest surface pressure and contains most of the plug cross-sectional area.

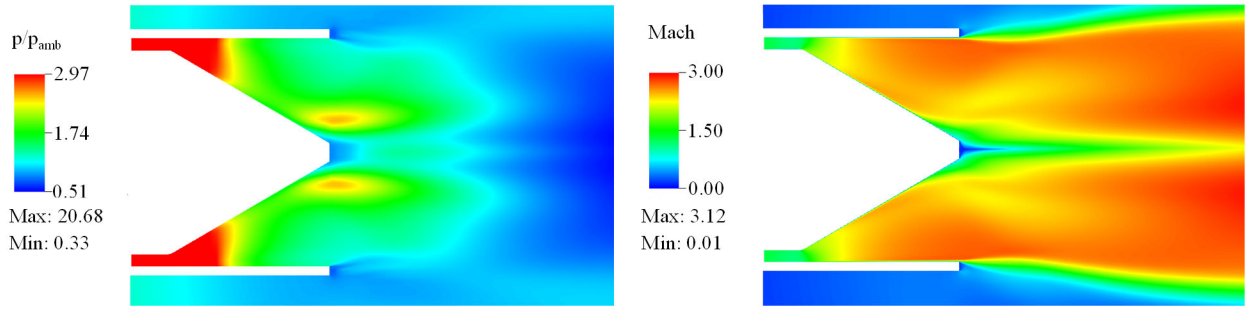

(a) **(b)**

Fig. 6 Time averaged contours of pressure (a) and Mach number (b) in the baseline nozzle configuration

III. Nozzle Optimization

Examination of the baseline nozzle flow field provided no specific information on how the performance could be improved. As such, a decision was made to perturb two general geometric parameters that influence shrouded plug nozzles. The first is the expansion area ratio, A_e/A_{ch}. The second is the degree to which the expansion area is split between the shroud surface and the cone. This is defined by the ratio A_{sh}/A_e. The shroud area, A_{sh} is illustrated below. The two parameters are not unrelated. A_e/A_{ch} cannot be increased without changing A_{sh}/A_e. However, A_{sh}/A_e can be changed while holding A_e/A_{ch} constant. Specifics of each parameterization are discussed separately in the following sections.

A. Expansion Area Variation

The four nozzles used in the expansion area study are shown in Fig. 7 along with their respective values of A_e/A_{ch} and A_{sh}/A_e and version designation. The physical dimensions shown are only those that differ from the baseline. Beginning with the baseline nozzle in the upper left of the figure and moving clockwise, the exit areas steadily increase. The plug portion of each nozzle and the overall length do not change. All of the exit area change is brought about by profiling the outer shroud as shown. The serpentine shape of the shroud inner wall is not based on theory. It is simply a smooth fit that transitions from the inner to the outer diameter with zero rate of change at the beginning and end. The additional exit area that it provides defines the shroud area, A_{sh}.

In order to focus specifically on the performance of the nozzle component, the nozzle thrust, F_n is defined as the difference between Eq. 1 and the thrust that the RDRE chamber produces without a nozzle.

$$F_n = F - F_{no\_nozzle} \tag{2}$$

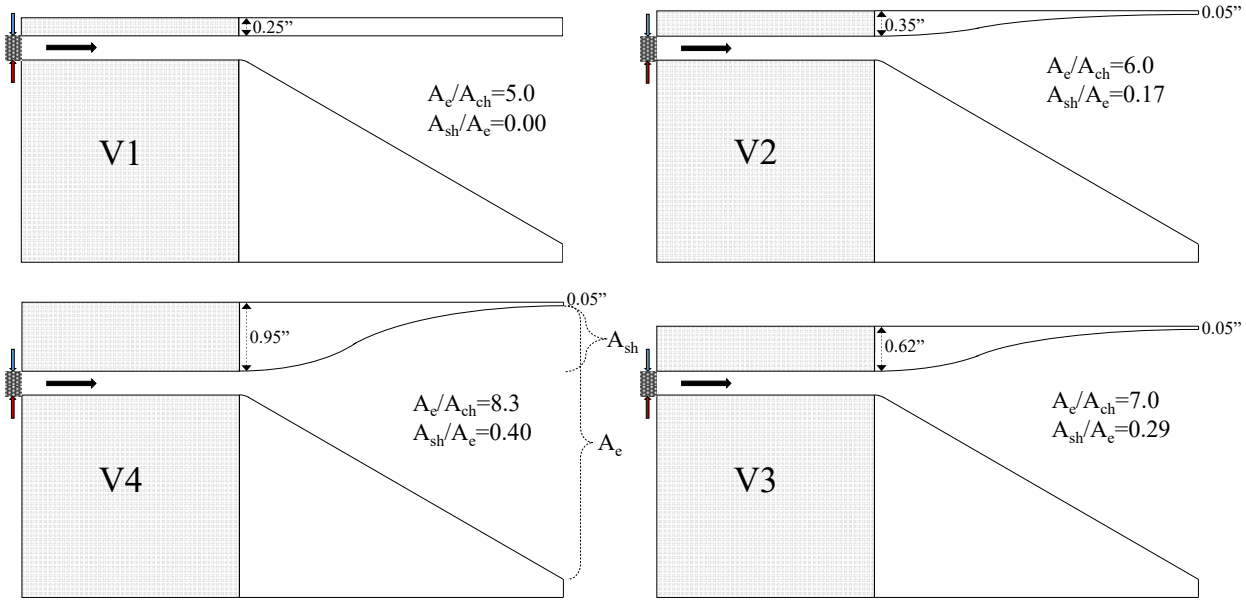

Fig. 7 Nozzle configurations used to study the impact of exit area variation

For the notional ideal nozzle, $F_{ni} = F_i - F_{no\_nozzle} = 1010$ lb$_f$.

The performance of the Fig. 7 nozzles is shown in Fig. 8. The nozzle thrust, plotted as a percentage of the ideal nozzle thrust, is presented as a function of the expansion area ratio, A_e/A_{ch}. Also shown is the percentage of the nozzle thrust that is produced by the time averaged exit pressure. Positive values indicate under expansion, negative values represent over expansion. The points on the far left represent the baseline nozzle. Both data sets have been fitted with a second order polynomial to indicate trends. Approximately 7% improvement in the thrust is obtained if A_e/A_{ch} is increased from 5 to 6.5. This appears to coincide with near perfect expansion of the flow on a time averaged basis which suggests that the improvement is mostly the result of having a properly matched nozzle for the expanding flow. However, it should be kept in mind that the value of A_{sh}/A_e is also changing here and it also impacts performance, as will be shown next.

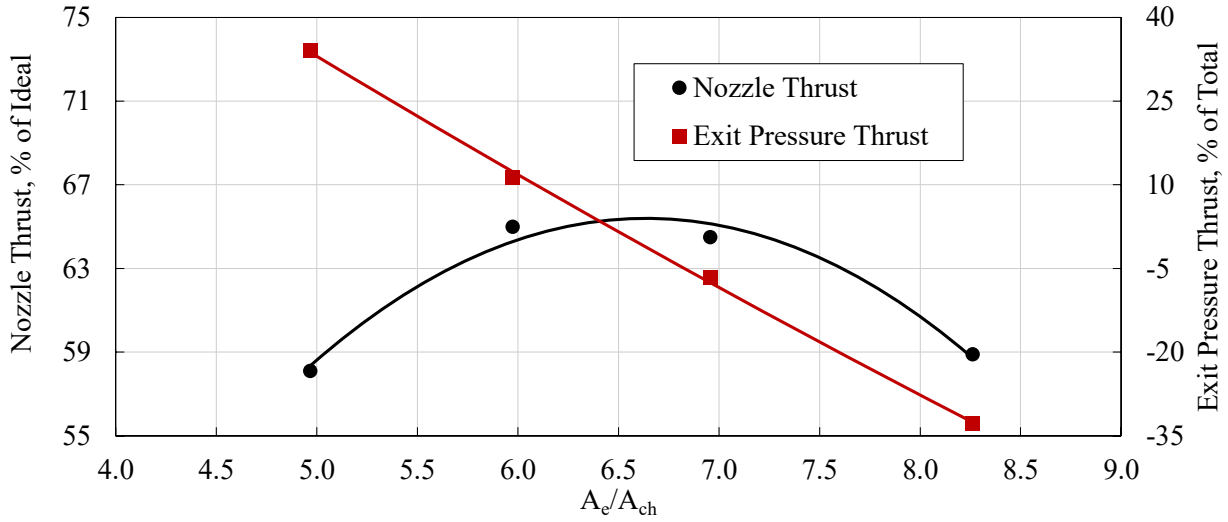

Fig. 8 Nozzle performance as a function of exit area ratio

B. Variation in Shroud Area at Constant Exit Area

The four nozzles used in the variable A_{sh} at constant A_e study are shown in Fig. 9 in similar fashion to Fig. 7. Beginning with the baseline nozzle in the upper left of the figure and moving clockwise, the ratio A_{sh}/A_e steadily increases. The performance of this nozzle series is shown in Fig. 10, in the same manner as Fig. 8, but with A_{sh}/A_e replacing A_e/A_{ch} as the independent variable. All four nozzles are slightly under expanded, but the three with $A_{sh}/A_e > 0$ are less so than the baseline. It is interesting that there is a difference in degree of under expansion given that the value of A_e/A_{ch} is the same for all four. However, it is noted that the well-known direct relationship between area and pressure expansion ratio is based on uniform, steady flow. This flow field is neither. The thrust produced from nozzle Versions 5-7 is significantly higher than the best of Versions 1-4. It is not obvious why there is a greater performance response to A_{sh}/A_e when compared to A_e/A_{ch}. One observation in this regard is that thrust production improves as it is shifted away from being produced on the plug surface, and toward being produce on the shroud inner surface. An observation is not an explanation however, and more study is needed to understand this result.

The highest performing nozzle of all those tested was Version 7 with a 13.4% thrust improvement over the baseline. However, it also had the largest value of A_{sh}/A_e. This implies a larger diameter nozzle with greater mass.

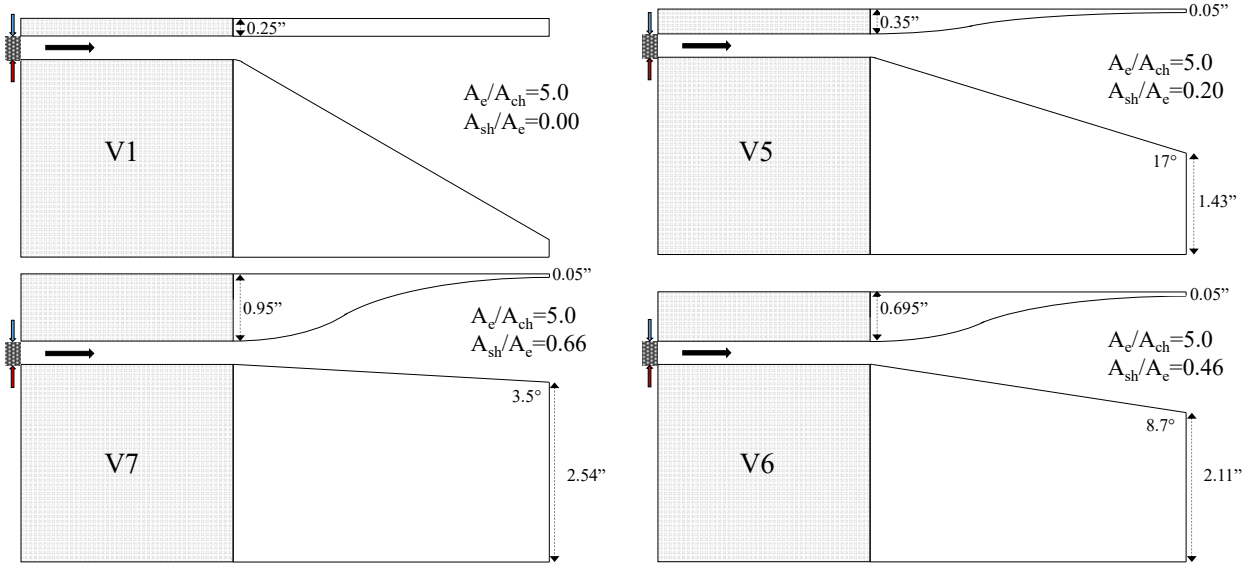

Fig. 9 Nozzle configurations used to study the impact of variation in shroud area with constant exit area

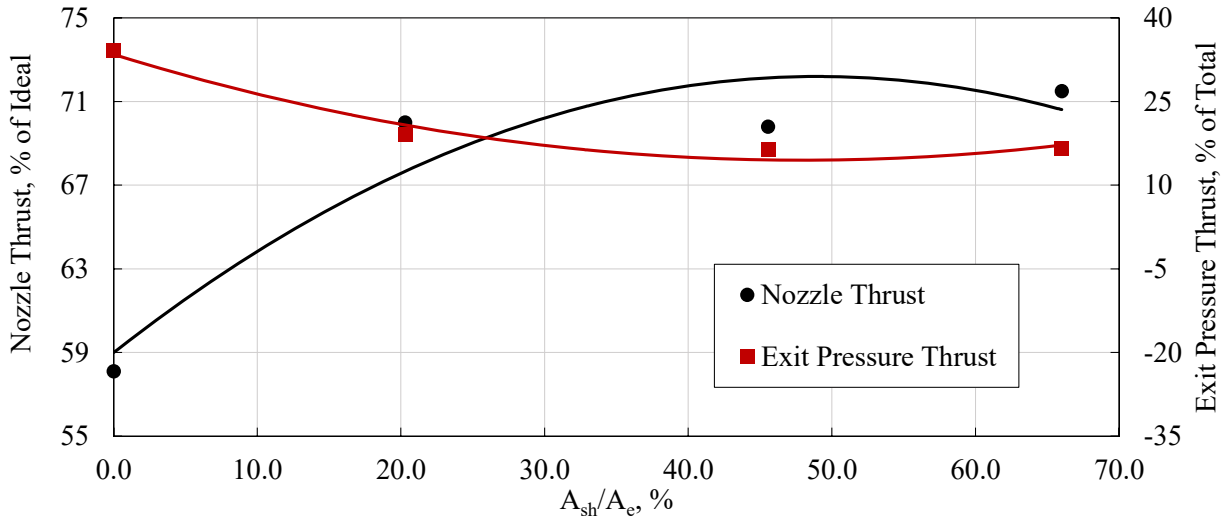

Fig. 10 Nozzle performance as a function of shroud area to exit area ratio with fixed expansion area ratio

Minimizing mass is a practical goal for any rocket engine, as mentioned earlier. Furthermore, minimizing outer diameter was a significant factor for the particular additive manufacturing process and equipment used to fabricate the experiment. Since the Version 5 nozzle was notably smaller in diameter, but just 1.5% lower in terms of nozzle thrust relative to ideal, it was selected as the recommended one for experimental testing.

The bluff body region of the Version 5 nozzle (i.e., the truncated portion of the plug) generated a drag force equivalent to -9.5% of the nozzle thrust (-1.4% of total thrust). It is possible that this small drag force could be eliminated by extending the plug to a point. However, this also adds material that must be actively cooled, and it adds mass. The small drag force was therefore deemed acceptable.

It is tempting to consider a nozzle design which combines the benefits of increasing A_{sh}/A_e, with those from using the seemingly correct A_e/A_{ch}=6.5 (see Fig. 8) to achieve full expansion. Although this exact configuration was not simulated, there was one with A_e/A_{ch}=5.7, A_{sh}/A_e=18%. The resulting nozzle thrust was actually 1.4% lower than the Version 5 nozzle, even though the exit pressure thrust fraction went from 19% to 10%. This result suggests that the parameters A_e/A_{ch} and A_{sh}/A_e are not independent.

Figures 11 and 12 are the equivalent of figures 5 and 6 for the optimized Version 5 nozzle. They show instantaneous contours of pressure, and time-averaged contours of pressure and Mach number, respectively in the nozzle flow field. As with the baseline nozzle it is seen that the flow is highly unsteady and spatially non-uniform throughout the nozzle interior. However, on a time averaged basis the flow is well-behaved and attached throughout the domain.

C. Grid Refinement

Due to time and resource restraints, a full grid refinement study was not possible. However, a simulation of the Version 5 nozzle was performed using a grid with approximately 7.7 million numerical cells (i.e. twice as many as in the rest of the study). The refinement was particularly concentrated in regions near walls where boundary layers and fluid separation might occur. The fifteen wave revolutions required for convergence took approximately 30 days, running on 480 cores. The results were indistinguishable from the original simulation, with the total predicted thrust matching the original to within 0.4%.

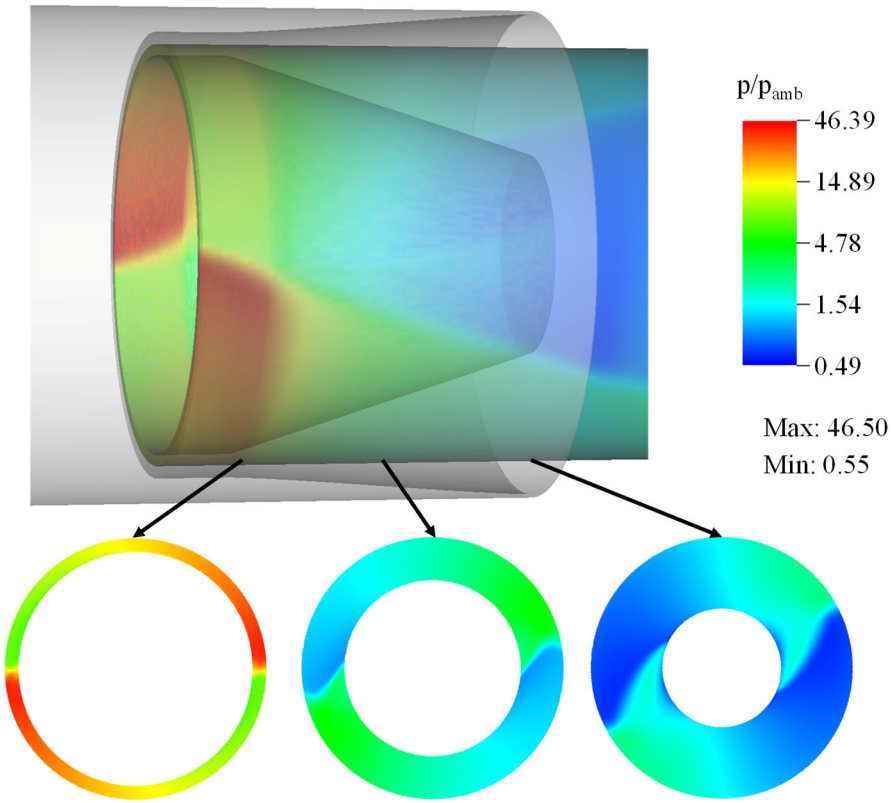

Fig. 11 Contours of pressure (log scale) at a moment in time for the optimized Version 5 nozzle during limit cycle operation

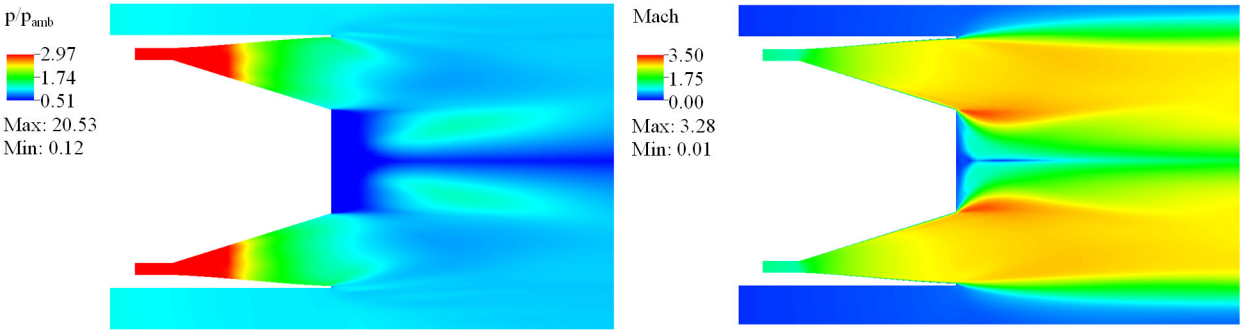

(a) **(b)**

Fig. 12 Time averaged contours of pressure (a) and Mach number (b) in the Version 5 nozzle configuration

IV. Discussion

Although improved nozzle performance was obtained by optimizing the shroud area, and although the baseline design was already showing overall RDRE-plus-nozzle thrust within 8.5% of the ideal value, the nozzle design and parameterization cannot be generalized. This investigation was conducted for a particular RDRE configuration, running a particular detonation cycle, at a single operating point. In this section, a few of the many possible differences in RDRE configuration and operational characteristics, and their implications, are briefly discussed.

If the current RDRE runs at a different flow rate than planned, or if the combustion process is markedly different than the rotating detonation cycle computed, then the nozzle will be off design. If it is under expanded (typical of higher mass flow rate), the nozzle may not be strongly affected. If it is over expanded, then significant nozzle performance degradation may occur. If the RDRE chamber operates with something other than 2 detonation waves, it is unclear how performance will be affected.

If a throat is added to the RDRE chamber, or the mean diameter is changed, or the channel width is altered, then the physical area available for expansion may be significantly different than what is called for fluidically. Depending on how this difference manifests, the baseline Version 1 shroud and plug configuration could prove inappropriate as a starting point for a design.

If the optimization objectives change from maximizing thrust to minimizing weight, or length, then even with the constraint of using a shrouded plug, the design may be surprisingly different than what is proposed here. Similarly, if an in-space RDRE application is under consideration, the optimal values of A_e/A_{ch} and A_{sh}/A_e could differ substantially from what was found here.

These and other considerations, for which there are no established guidelines for RDREs, highlight the value of a computational methodology such as the one utilized for this work and detailed in Ref. 5. A validated simulation, utilizing modest computational resources, can be exercised on multiple nozzle configurations, to find the one best suited for a given application. This process can save resources that would otherwise be devoted to fabricating and testing multiple nozzle builds.

V. Conclusion

The nozzle for a laboratory rotating detonation rocket engine (RDRE) was designed using a three-dimensional computational fluid dynamic simulation supplied with unsteady boundary conditions representing the upstream RDRE combustor. The primary design objective was to optimize nozzle thrust at a particular operating point defined by propellant flow rates and successful detonation. A baseline shrouded and truncated plug nozzle configuration served as a starting point. The overall nozzle area expansion ratio and the fraction of the expansion area provided by the shroud were chosen as free parameters with which to maximize performance. These two parameters impact the angle of the plug nozzle cone, and the bluff body area associated with its truncation. Nozzle thrust was isolated by measuring the difference between the thrust of the RDRE chamber-plus-nozzle combination and that of the chamber alone (which was choked at the nozzle entrance). The baseline nozzle was found to perform well, yielding 58.1% of the thrust calculated for a notional ideal RDRE nozzle which can instantaneously change shape to allow isentropic expansion of every fluid element. The total thrust of the RDRE chamber-plus-baseline nozzle combination was 91.5% of the ideal total thrust. Optimization improved the performance, bringing the nozzle thrust to 70.0% of the ideal, and total engine thrust (chamber-plus-nozzle) to 94% of the ideal. The fraction of the expansion area provided by the shroud showed

a much stronger impact on nozzle performance than did overall nozzle area ratio. The analysis presented in this study demonstrates that numerical simulations are useful tools for improving the design and performance of RDRE nozzles.

References

[1] Lietz, C., Ross, M., Desai, Y., and Hargus, W.A., "Numerical Investigation of Operational Performance in a Methane-Oxygen Rotating Detonation Rocket Engine," AIAA-2020-0687, January, 2020.

[2] Paxson, D.E., "Numerical Analysis of a Rotating Detonation Engine in the Relative Reference Frame," AIAA-2014-0284, January, 2014, also NASA/TM 2014-216634, 2014.

[3] Angelino, G., "Approximate Method for Plug Nozzle Design," *AIAA Journal*, Vol. 2, No. 10, 1964, pp.5

[4] Onofri, M., "Plug Nozzles: Summary of Flow Features and Engine Performance," AIAA-2002-0584, January, 2002

[5] Miki, K., Paxson, D.E., Perkins, H.D. and Yungster, S., "RDE Nozzle Computational Design Methodology Development and Application," AIAA-2020-3872, August, 2020.

[6] Paxson, D.E., Fotia, M.L., Hoke, J. L., Schauer, F. R., "Comparison of Numerically Simulated and Experimentally Measured Performance of a Rotating Detonation Engine," AIAA-2015-1101, January, 2015.

[7] Rankin, B., Fotia, M. L., Paxson, D. E., Hoke, J. L., Schauer, F. R., "Experimental and Numerical Evaluation of Pressure Gain Combustion in a Rotating Detonation Engine," AIAA-2015-0877, January, 2015.

[8] Tobias, J., Agrawal, A. K., Paxson, D. E., "Experimental and Computational Analysis of a Rotating Detonation Combustor," AIAA-2022-1879, January, 2022.

[9] Theuerkauf, S. W., Schauer, F. R., Anthony, R. J., Paxson, D. E., Stevens, C. A. Hoke, J. L., "Comparison of Simulated and Measured Instantaneous Heat Flux in a Rotating Detonation Engine," AIAA-2016-1200, January, 2016.

[10] Stubbs, R., and Liu, N.-S., "Preview of the National Combustion Code,", AIAA-1997-3114, July, 1997.

[11] Teasley, T., Williams, B., Larkey, A., Protz, C., Gradl, P., "A Review Towards the Design Optimization of High-Performance Additively Manufactured Rotating Detonation Rocket Engine Injectors," AIAA-2021-3655, August, 2021.

[12] Kaemming, T. A., Paxson, D. E., "Determining the Pressure Gain of Pressure Gain Combustion," AIAA-2018-4567, July, 2018.

[13] Paxson, D.E., Perkins, H.D., "A Simple Model for Rotating Detonation Rocket Engine Sizing and Performance Estimates," AIAA-2021-0192, January, 2021.

[14] Gordon, S. and McBride, B., "Computer Program for Calculation of Complex Chemical Equilibrium Compositions and Applications," NASA RP-1311, October, 1994.

[15] Miki, K., Moder, J., and Liou, M.-S., "Enhancing Open National Combustion Code and Application of Energy Efficient Engine Combustor," *Journal of Propulsion and Power*, Vol. 34, 2018, pp. 415-427.

[16] Thompson, P. A, Compressible Fluid Dynamics, McGraw-Hill, 1988, pp. 281.